



Contents lists available at ScienceDirect

## Planetary and Space Science

journal homepage: [www.elsevier.com/locate/pss](http://www.elsevier.com/locate/pss)

## A survey of southern hemisphere meteor showers

Peter Jenniskens<sup>a,b,\*</sup>, Jack Baggaley<sup>c</sup>, Ian Crumpton<sup>c</sup>, Peter Aldous<sup>c</sup>, Petr Pokorný<sup>d</sup>,  
Diego Janches<sup>d</sup>, Peter S. Gural<sup>a</sup>, Dave Samuels<sup>a</sup>, Jim Albers<sup>a</sup>, Andreas Howell<sup>a</sup>,  
Carl Johannink<sup>a</sup>, Martin Breukers<sup>a</sup>, Mohammad Odeh<sup>e</sup>, Nicholas Moskovitz<sup>f</sup>, Jack Collison<sup>a,g</sup>,  
Siddha Ganju<sup>a,g</sup>

<sup>a</sup> SETI Institute, 189 Bernardo Ave, Mountain View, CA, 94043, USA<sup>b</sup> NASA Ames Research Center, Mail Stop 241-11, Moffett Field, CA, 94035, USA<sup>c</sup> Dept. of Physics and Astronomy, University of Canterbury, Christchurch, 8140, New Zealand<sup>d</sup> NASA Goddard Space Flight Center, 8800 Greenbelt Rd, Greenbelt, MD, 20771, USA<sup>e</sup> International Astronomical Center, P.O. Box 224, Abu-Dhabi, United Arab Emirates<sup>f</sup> Lowell Observatory, 1400 West Mars Hill Road, Flagstaff, AZ, 86001, USA<sup>g</sup> NASA Frontier Development Lab, USA

## ARTICLE INFO

## Keywords:

Meteor  
Meteor shower  
Meteoroid orbit  
Comet  
Southern hemisphere  
Shower lookup table

## ABSTRACT

Results are presented from a video-based meteoroid orbit survey conducted in New Zealand between Sept. 2014 and Dec. 2016, which netted 24,906 orbits from +5 to –5 magnitude meteors. 44 new southern hemisphere meteor showers are identified after combining this data with that of other video-based networks. Results are compared to showers reported from recent radar-based surveys. We find that video cameras and radar often see different showers and sometimes measure different semi-major axis distributions for the same meteoroid stream. For identifying showers in sparse daily orbit data, a shower look-up table of radiant position and speed as a function of time was created. This can replace the commonly used method of identifying showers from a set of mean orbital elements by using a discriminant criterion, which does not fully describe the distribution of meteor shower radiants over time.

## 1. Introduction

Meteor showers identify streams of meteoroids that approach from a similar direction and presumably originated from the same parent object (Jenniskens, 2017). In recent years, over 300 meteor showers have been identified, of which 112 have been established and are certain to exist. A Working List of identified showers is maintained by the IAU Meteor Data Center (Jopek and Kanuchova, 2017).

The southern hemisphere meteor showers are not as well mapped as those on the northern hemisphere. Only 27 out of 112 established showers have negative declinations. The first of these showers, such as the Phoenicids (IAU#256, PHO), were initially identified by visual observers in South Africa, Australia and New Zealand. Early visual observations were summarized by Ronald Alexander McIntosh (1904–1977), an amateur astronomer and journalist with the New Zealand Herald. His 1935 paper “An index to southern hemisphere meteor showers” identified 320 showers derived from visually plotted meteor paths on star

charts (Fig. 1A). However, many proposed showers were defined by a statistically unreliable grouping of meteor tracks traced to a diffuse radiant.

Southern hemisphere showers were mapped by radar, starting in the late 1950's, by W. Graham Elford and his students Alan A. Weiss and Carl Nilsson at Adelaide in Australia (Weiss, 1955, 1960a, b; Nilsson, 1964; Gatrell and Elford, 1975). More recently, a new type of meteor radar was developed in Adelaide, which are now deployed at many locations around the globe. Single-station derived southern hemisphere meteor shower radiants were published by Younger et al. (2009). A history of the Adelaide group is given in Reid and Younger (2016). At the same time, Clifford D. Ellyett and his student Colin S. Keay observed meteors by radar in Christchurch, New Zealand (Ellyett and Keay, 1956; Ellyett et al., 1961). Keay continued observations from Newcastle, Australia (Rogers and Keay, 1993). In the 1990's, the AMOR radar in Christchurch, New Zealand, provided orbital data for the six strongest meteor showers (Galligan, 2001, 2003; Galligan and Baggaley, 2004, 2005).

\* Corresponding author. SETI Institute, 189 Bernardo Ave, Mountain View, CA, 94043, USA.

E-mail addresses: [petrus.m.jenniskens@nasa.gov](mailto:petrus.m.jenniskens@nasa.gov) (P. Jenniskens), [jack.baggaley@canterbury.ac.nz](mailto:jack.baggaley@canterbury.ac.nz) (J. Baggaley).

<https://doi.org/10.1016/j.pss.2018.02.013>

Received 25 October 2017; Received in revised form 4 February 2018; Accepted 16 February 2018

Available online xxxx

0032-0633/© 2018 Published by Elsevier Ltd.

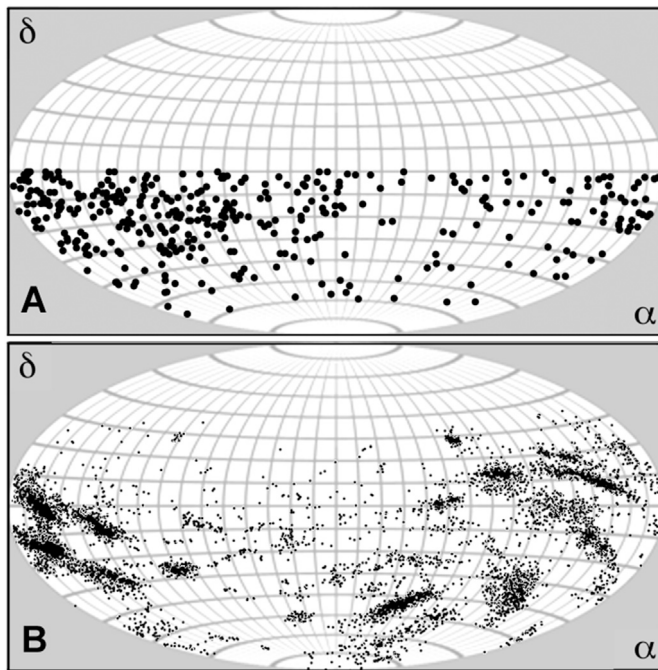


Fig. 1. (A) McIntosh (1935) identified these radiant positions of showers throughout the year, shown as geocentric Right Ascension and Declination coordinates in Hammer-Aitoff projection. (B) The radiant position of shower-assigned meteors in CAMS New Zealand data.

We report here on results from a CAMS-type video-based meteoroid orbit survey (Jenniskens et al., 2011) conducted in New Zealand in 2014–2016. The capability of the technique was demonstrated in earlier small scale video-based meteoroid orbit surveys in the southern hemisphere (e.g., Jopek et al., 2010; Molau and Kerr, 2014). The newly detected showers are compared to recent results from a southern hemisphere radar orbital survey conducted with the *Southern Argentina Agile Meteor Radar* (SAAMER) (Pokorny et al., 2017). It is found that video-based and radar-based observations detect, in general, different streams.

## 2. Methods

The CAMS New Zealand camera network consists of two stations at Geraldine (171.24155°E, 44.08756°S, +143m) and West Melton (172.40738°E, 43.49901°S, +78m). The Geraldine station is operated by Peter Aldous, the West Melton station by Ian Crumpton. Each station has 16 Watec Wat 902H2 Ultimate cameras with Pentax f1.2/12 mm lenses for a  $20 \times 30^\circ$  field of view. Video is recorded at 30 frames per second and  $640 \times 480$  pixel resolution (NTSC format). The video is compressed into Four Frame format files, preserving for each pixel in a given set of 256 frames the peak brightness value, the frame number that contained that peak brightness, the standard deviation of brightness and the average brightness. The field of view is calibrated against background stars, moving objects detected, and their astrometric data transmitted to the SETI Institute. At the Institute, tracks from both stations are triangulated and the radiant and speed of the trajectory at the initial detected point determined, using a Jacchia & Whipple type deceleration profile (Jenniskens et al., 2011).

The network has been in operation since September 11, 2014. At the end of December 2016, a total of 24,906 meteor trajectories had been measured of a quality better than  $1^\circ$  in radiant position (direction of the velocity vector) and better than 10% in entry speed. 20,527 of these (82%) have a negative (southern) geocentric declination. The peak brightness of the meteors ranged from about  $-5$  to  $+5$  magnitude, peaking at a visual magnitude of  $+1.6$  with a dispersion FWHM = 2.8

magnitudes. Meteors brighter than  $+0.5$  magn. were distributed exponentially with a magnitude distribution index of  $2.60 \pm 0.05$  (both shower and sporadic meteors), while fainter meteors were detected with fractional probability  $P(+1) = 0.77$ ,  $P(+2) = 0.34$ ,  $P(+3) = 0.069$ ,  $P(+4) = 0.0048$ , and  $P(+5) = 0.00005$ , assuming the actual distribution continued that exponential slope to fainter magnitudes.

The results from the New Zealand network were combined with those from all other (northern hemisphere) CAMS networks obtained by the end of 2016 (471,580 orbits total). CAMS California observations, for example, can detect meteors with radiants down to  $-37^\circ$  declination. After plotting all radiant positions in sun-centered ecliptic coordinates for short intervals of 5-degree solar longitude and 5-km/s entry speed, meteor showers were extracted by isolating clusters in radiant density using a very simple visual approach to defining the density cluster contour (Jenniskens et al., 2016a). First the established showers were identified, then known showers that have not yet been established. Finally, the remaining such clusters were identified as new showers. Compared to the sporadic background, the meteor radiant spatial density per square degree of sky was typically  $\geq 5$  times higher within the cluster  $2\sigma$  contour than that of the sporadic background (Jenniskens et al., 2016a).

Subsequently, the effort was repeated for the combined dataset with all published data from other video-based meteor orbit surveys, all of which detect meteors of similar brightness (992,220 orbits total). Those included data from the SonotaCo network during 2007–2016, the Edmond network during 2001–2015, and the Croatian Meteor Network during 2007–2013.

## 3. Results

The distribution of shower-assigned meteors in the CAMS New Zealand data is shown in Fig. 1B. Some previously reported meteor showers from southern hemisphere radar surveys are now confirmed. The delta Mensids (#130, DME), for example, were nicely observed by CAMS New Zealand, as previously reported (Jenniskens et al., 2016b).

One of the newly detected showers, the A Carinids (#842, CRN), is shown in Fig. 2. The figure shows a screen shot of the new public website at <http://cams.seti.org/FDL/>, created to display CAMS-detected meteors in near-real time. The data pertain to one date (October 12), and combines the results from all CAMS networks in the years 2010–2016.

The tool plots measured radiant positions on a rotatable sphere. Each colored position is a meteor that was assigned to a meteor shower using a look-up table. Color indicates the mean geocentric speed of meteor showers on an analog scale, with slow meteor showers in purple and blue, those with intermediate velocities in green, yellow, and orange, and fast showers in red. By hovering the mouse over a data point, a label will display the shower number (“0” if sporadic), while a separate box will show the geocentric entry speed of that meteor, as well as the solar longitude (time) and the sun-centered ecliptic radiant coordinates (Fig. 2). By clicking on the point, the meteor shower to which that meteor was assigned is now displayed in a planetarium program to illustrate the orbital elements of the meteoroid stream responsible (based on 2010–2016 CAMS data). Sporadic meteors (not assigned to a shower) are displayed in white.

Because the meteoroid streams evolve dynamically, and depending on the Earth’s orbital motion through the stream, showers tend to be active for several days, some up to several months. The shower lookup table aims to accurately record the duration of the stream and the motion of the radiant over time, as well as the radiant and velocity dispersion and its variations over time. The look-up table (see Appendix) was created by simply isolating the columns for solar longitude, sun-centered ecliptic radiant coordinates, geocentric entry speed and IAU shower number from the shower-assigned combined 992,220-orbit database.

While creating the look-up table, a large number of new showers were detected. Table 1 lists the newly detected showers from CAMS data alone. 21 new southern hemisphere showers were detected, as well as a number

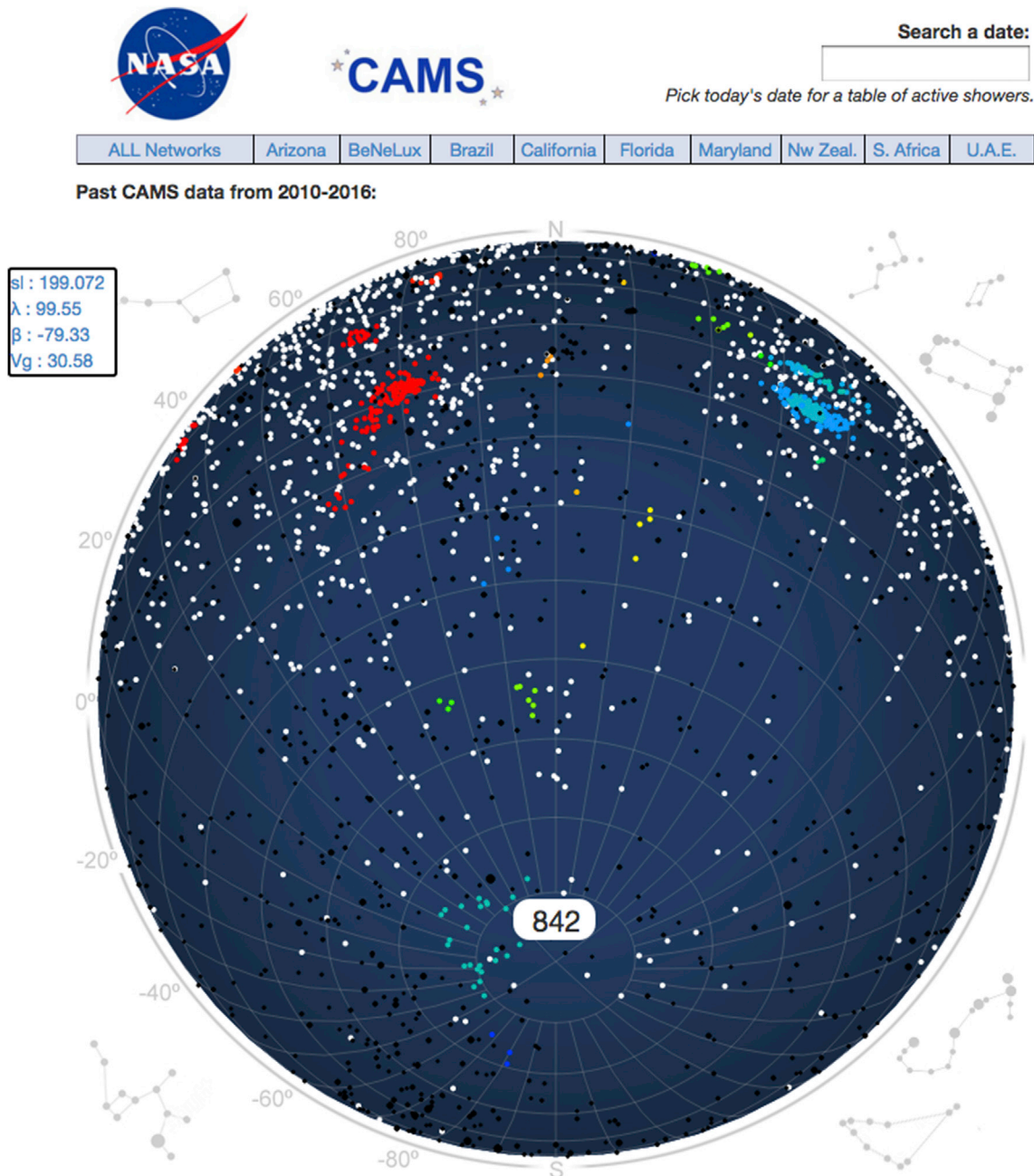


**Fig. 2.** CAMS data visualization for combined (all networks) results from October 12 (2010–2016). Each point is a triangulated meteor, color coded when assigned to a meteor shower. Red are fast 65–72 km/s meteors, blue are slow 11–20 km/s meteors. New shower 842 is marked as when hovering with cursor. Data for the meteor to which cursor points is marked. (For interpretation of the references to color in this figure legend, the reader is referred to the Web version of this article.)

of northern hemisphere showers. These average orbital elements were reported to the IAU Meteor Data Center and are included in the Working List of Meteor Showers (#822–860). We include cases where the number of meteors is small ( $N < 8$  in Table 1), but these streams are compact and stand out well from the sporadic background.

Table 2 lists the additional showers identified in the combined dataset, which includes another 21 southern declination showers. The average orbital elements presented in Table 2 are those of the CAMS-detected meteors only. The tally of all meteors is also given, showing that some meteor showers are more prominently detected in other surveys due to observing conditions or shower activity variations.

Finally, Table 3 lists 21 showers (including 2 at negative declination) that were tentatively detected in early CAMS data and reported to the Meteor Data Center, but were not included in the publication on showers 621–750 (Jenniskens et al., 2016a). Now that these same showers were

detected from a larger dataset, they were added to the Working List and given the same IAU number as previously assigned. In addition to that, the mean orbit of all previously detected showers were added to the MDC database.

In checking to avoid duplicates, we noticed that a few showers were close to previously reported showers that were not recovered. In particular, shower 870 (JPG) is near 433 (ETP), but has a 51.5 km/s entry speed instead of 34.5 km/s. Shower 887 (DZB) is only  $6^\circ$  higher in declination and 6 km/s slower than shower 731 (JZB). Shower 920 (XSC) is  $8^\circ$  higher in declination and 9 km/s lower in entry speed than shower 140 (XLI). And shower 923 (FBO) is nearby 138 (ABO) but has a 7 km/s higher entry speed.

In all, 20.8% of meteors in the CAMS New Zealand dataset were assigned to meteor showers. Some showers are not seen in all years. The web tool creates a separate tab with the combined past data from 2010 to

**Table 1**

New meteor showers identified in CAMS data. For each shower the mean solar longitude (J2000), geocentric coordinates of the radiant, the geocentric entry speed ( $V_g$ ), semi-major axis ( $a$ ), perihelion distance ( $q$ ), eccentricity ( $e$ ), argument of perihelion ( $\omega$ ), longitude of the ascending node ( $\Omega$ ) and inclination ( $i$ ) are given, as well as the total number of meteors detected for that shower.

#	IAU	Name	Sol. (°)	RAg (°)	DECg (°)	$V_g$ (km/s)	$a$ (AU)	$q$ (AU)	$e$	$\omega$ (°)	$\Omega$ (°)	$i$ (°)	$N$
822	NUT	nu Taurids	123.3	64.3	1.6	61.8	16.6	0.520	0.970	270.4	303.3	136.5	40
823	FCE	56 Cetids	163.9	28.9	-22.9	44.8	9.91	0.376	0.963	106.3	343.9	70.2	98
824	DEX	Dec. Sextantids	268.3	159.7	-4.5	69.3	23.9	0.797	0.970	52.4	88.3	157.6	19
825	XIE	xi Eridanids	196.1	66.6	-5.8	54.6	72.3	0.370	0.996	105.2	16.1	103.7	16
826	ILI	iota1 Librids	37.1	228.3	-21.3	32.1	2.46	0.284	0.885	122.1	217.1	4.9	56
827	NPE	nu Pegasids	28.9	329.2	2.9	61.8	999	0.370	1.004	74.8	28.9	142.9	44
828	TPG	31 Pegasids	5.9	334.4	13.0	42.3	24.3	0.244	0.990	58.8	5.9	49.5	4*
829	JSP	July 77 Pegasids	110.0	355.1	9.4	66.3	14.9	0.684	0.956	250.8	110.0	159.0	31
830	SCY	63 Cygnids	94.4	317.1	50.9	44.4	9.34	0.998	0.893	195.8	94.4	76.9	57
831	GPG	gamma Pegasids	140.1	4.1	14.1	57.4	10.7	0.178	0.984	311.5	140.0	139.8	23
832	LEP	Leporids	169.3	89.9	-26.0	52.7	8.26	0.979	0.882	342.2	349.3	95.9	64
833	KOR	kappa Orionids	223.1	89.2	-7.8	52.4	17.8	0.416	0.977	100.1	43.1	94.6	31
834	ACU	April $\theta$ Centaurids	21.0	210.5	-37.4	41.0	26.8	0.304	0.989	113.7	201.0	44.9	8
835	JDP	June $\delta$ Pavonids	82.1	295.9	-63.3	39.2	27.1	0.581	0.979	82.2	262.1	55.5	11
836	ABH	April $\beta$ Herculis	20.3	249.7	23.0	47.5	31.3	0.659	0.980	252.1	20.3	78.7	8
837	CAE	Caelids	205.8	69.1	-39.4	37.9	999	0.841	1.010	46.5	25.8	58.1	8
838	ODS	Oct. $\delta$ Sextantids	212.1	160.7	-3.7	59.2	47.1	0.174	0.997	229.3	32.1	140.1	10
839	PSR	phi Serpentids	25.1	242.2	14.0	46.3	999	0.435	1.017	277.2	25.1	69.9	5*
840	TER	tau4 Eridanids	169.0	49.3	-24.5	50.3	23.1	0.628	0.973	76.3	349.0	88.5	13
841	DHE	delta Herculis	19.5	256.2	23.7	49.5	13.7	0.745	0.947	241.8	19.5	85.6	32
842	CRN	A Carinids	198.0	103.2	-57.0	30.1	2.87	0.989	0.655	354.7	18.0	50.4	121
843	DMD	Dec. $\mu$ Draconids	277.9	258.5	57.9	27.4	2.60	0.973	0.626	166.8	277.9	45.0	39
844	DTP	Dec. $\theta$ Pyxidids	249.6	138.8	-25.4	60.6	38.2	0.956	0.975	20.3	69.6	113.1	28
845	OEV	Oct. $\eta$ Virginids	211.5	181.6	-7.5	40.7	2.47	0.089	0.964	210.9	31.5	21.5	5*
846	TSC	tau Sculptorids	85.0	21.0	-27.4	61.0	10.6	0.936	0.912	326.6	265.0	121.5	5*
847	BEL	beta Leonids	218.8	179.4	17.3	57.4	36.7	0.190	0.995	51.4	218.8	123.0	22
848	OPE	omicron Perseids	198.1	53.5	31.5	51.7	6.20	0.071	0.989	330.3	198.1	106.0	11
849	SZE	Sep. $\zeta$ Eridanids	172.5	48.2	-8.1	56.9	999	0.389	1.007	102.9	352.5	113.2	17
850	MBA	May $\beta$ Aquariids	74.3	323.3	-3.1	68.3	999	0.740	1.051	242.0	74.3	159.3	3*
851	BEC	beta Carinids	170.2	139.8	-73.9	17.7	2.85	0.999	0.650	350.8	350.2	26.2	21
852	AST	alpha Sculptorids	74.5	17.2	-29.4	61.7	999	0.867	1.065	315.9	254.5	119.7	7*†
853	ZPA	zeta Pavonids	1.1	277.8	-71.7	55.1	25.5	0.994	0.961	354.1	181.1	99.2	5*
854	PCY	psi Cygnids	53.8	297.5	54.3	39.3	17.2	1.008	0.941	174.7	53.8	65.0	32
855	ATD	Aug. $\tau$ Draconids	138.3	296.9	74.8	33.1	4.75	1.013	0.787	178.4	138.3	55.1	10
856	EMO	$\epsilon$ Monocerotids	158.7	95.4	2.0	62.3	11.6	0.588	0.950	278.2	338.6	134.5	26
857	EVO	eta Volantids	197.9	134.6	-74.3	19.9	2.89	0.979	0.661	344.3	17.9	29.8	55
858	FPB	February $\phi$ Bootids	312.6	235.4	40.6	47.5	6.11	0.976	0.840	187.8	312.6	82.7	59
859	MTB	March 12 Bootids	344.1	212.6	26.6	46.5	24.3	0.481	0.980	272.3	344.1	72.7	15
860	PAN	$\phi$ Andromedids	71.6	355.9	46.5	49.9	13.9	0.695	0.951	110.6	71.6	88.9	14

Notes: \* Compact shower; † Data from 2016, not including 3 meteors detected in 2015 at Solar longitude = 70.7, RAg = 14.3°, DECg = -31.6° and  $V_g$  = 61.9 km/s.

2016, making it possible to compare newly collected data to that from past observations.

Irregular (non-annual) showers are called meteor outburst. One notable meteor outburst was the Volantid shower detected on New Year's eve 2015 (Fig. 3). CAMS detected 21 Jupiter family comet like meteoroids from the constellation Volans (the flying fish) out of 59 total detected meteoroids, standing out as a significant enhancement over local sporadic activity (Jenniskens et al., 2016c). Meteor radar data in Buckland Park Australia and at Davis Station in Antarctica recorded the outburst as well (Younger et al., 2016). That data showed that the shower was active on Dec 31, January 1 and January 2 (Fig. 3B). It was not seen in previous years and was not detected in early 2017. The shower contained some bright meteors. Even the Desert Fireball Network detected this shower (Fig. 3C).

#### 4. Discussion

With these additional 44 southern hemisphere showers added, there are now 135 CAMS-detected showers and shower components that have southern declinations, while 362 showers have northern declinations. If the actual shower distribution is symmetrical, this suggests that another ~200 meteor showers remain to be discovered in the southern hemisphere down to the sensitivity level of current northern hemisphere CAMS surveys.

#### 4.1. Video versus radar detected showers

The video-detected showers can be compared to recent results reported from the ongoing SAAMER radar orbital survey program in southern Argentina. The system characteristics are described in detail in Janches et al. (2015) and the latest survey results were reported by Pokorný et al. (2017). Of 58 detected showers, 34 were newly reported (IAU showers #759–792). Of the newly reported showers, 7 were detected in CAMS data (##768, 771, 783–786 and 792). Mean orbital elements for such showers confirmed in CAMS data were submitted to the Meteor Data Center.

Most SAAMER showers are located in the southern toroidal ring, which is a source region that surrounds the apex source, in between the apex and antihelion/helion sources (Campbell-Brown, 2008). The new showers include several that are on the inside of the helion/antihelion sources, all having low perihelion distances. The slightly less sensitive Canadian Meteor Orbit Radar (CMOR) in the northern hemisphere also detected many northern toroidal ring showers (Brown et al., 2010). Brown et al. concluded from their similar orbital secular invariants  $U = \sqrt{(3-T_j)}$  and  $\cos(\Theta)$ , with  $\Theta$  the angle between radiant and the apex direction of Earth's motion and  $T_j$  the Tisserand parameter with respect to Jupiter (Valsecchi et al., 1999), that many of these detected showers belonged to seven evolved shower complexes.

Fig. 4 shows two of the SAAMER-detected showers in the solar

Table 2

New meteor showers identified in combined CAMS, SonotaCo, Edmond and CMN data. Mean elements are given for CAMS data only, based on the number of meteors N. Total number of meteors in all networks: Nt.

#	IAU	Name	Sol. (°)	RAg (°)	DECg (°)	Vg (km/s)	a (AU)	q (AU)	e	$\omega$ (°)	$\Omega$ (°)	i (°)	N	Nt
862	SSR	16 Scorpiids	362.2	242.6	-7.2	62.7	6.96	0.427	0.941	280.5	362.2	147.2	26	65
863	TLR	12 Lacertids	79.1	338.9	41.3	54.9	12.1	0.971	0.921	155.3	79.1	101.9	10	16
864	JSG	June 66 Pegasids	82.1	350.3	13.0	67.6	7.68	0.999	0.870	164.6	82.1	152.6	8	14
865	JES	June $\epsilon$ Serpent.	87.9	239.1	4.5	12.9	2.51	0.924	0.631	220.1	88.0	8.5	19	23
866	ECB	$\epsilon$ Coronae Borealids	107.4	238.7	26.0	11.3	2.43	0.998	0.589	197.4	107.4	12.4	16	28
867	FPE	52 Pegasids	96.7	345.5	11.6	66.8	19.2	0.840	0.957	229.9	96.6	149.9	8	14
868	PSQ	psi3 Aquariids	120.5	347.4	-11.9	53.1	5.01	0.048	0.991	156.4	300.5	140.7	11	29
869	UCA	upsilon1 Cassiopeiids	124.9	9.3	59.6	53.5	14.0	1.010	0.928	171.7	124.9	97.5	10	53
870	JPG	July $\eta$ Pegasids	128.1	339.9	33.5	51.5	258.	0.594	1.000	260.3	128.1	91.8	12	33
871	DCD	delta Cepheids	122.9	345.9	56.7	49.9	25.9	0.995	0.961	196.5	122.9	88.2	7	17
872	ETR	$\epsilon$ Triangulids	137.6	27.6	33.9	66.7	20.8	0.945	0.955	210.7	137.6	143.2	8	30
873	OMI	omicron Cetids	152.8	39.9	-6.4	61.9	14.7	0.563	0.965	84.6	332.8	134.8	5	28
874	PXS	Sep. xi Perseids	174.8	59.8	37.9	66.5	263.	0.739	0.998	242.0	174.8	147.4	18	37
875	TEI	tau9 Eridanids	192.3	61.4	-18.8	47.7	15.3	0.528	0.968	87.7	12.3	80.4	71	117
876	ROR	rho Orionids	185.3	78.7	4.1	66.2	22.7	0.788	0.965	55.7	5.3	144.6	18	38
877	OHD	omega Hydrids	205.7	142.2	7.7	67.0	999	0.524	1.015	273.1	25.7	164.9	16	42
878	OEA	Oct. $\epsilon$ Aurigids	207.7	73.4	45.3	56.0	11.2	0.313	0.973	293.1	207.7	113.9	8	20
879	ATI	alpha Taurids	203.3	72.4	15.2	58.1	9.36	0.142	0.985	136.8	23.3	152.9	18	38
880	YDR	Y Draconids	206.3	146.4	76.4	47.6	5.92	0.990	0.833	188.7	206.3	84.0	16	50
881	TLE	theta Leonids	218.7	165.8	12.7	62.4	6.85	0.299	0.958	64.5	218.7	163.0	14	24
882	PLE	phi Leonids	232.5	172.1	-4.3	64.0	14.6	0.351	0.979	252.1	52.5	161.7	10	22
883	NMD	Nov. $\mu$ Draconids	227.3	253.6	55.8	23.0	2.40	0.968	0.597	160.0	227.3	36.8	6	12
884	NBP	Nov. $\beta$ Pyxidids	240.8	128.1	-35.0	52.2	8.44	0.978	0.884	11.7	60.8	93.0	9	21
885	DEV	Dec. $\epsilon$ Virginids	277.6	198.6	10.4	67.9	4.72	0.957	0.798	159.9	277.6	150.1	6	26
886	ACV	alpha Corvids	283.4	184.9	-29.8	64.2	3.22	0.972	0.698	346.7	103.4	135.3	16	32
887	DZB	Dec. $\zeta$ Bootids	279.7	222.6	14.7	58.4	3.49	0.646	0.817	103.7	279.7	118.5	4	26
888	SCV	6 Corvids	296.4	185.8	-31.4	64.0	3.74	0.941	0.748	25.9	116.4	133.1	12	16
889	YOP	Y Ophiuchids	313.9	265.8	-5.5	57.5	30.1	0.234	0.994	57.8	313.9	121.1	7	15
890	ESU	eta Scutids	335.1	283.5	-7.4	58.3	9.55	0.239	0.975	57.5	335.1	131.4	6	20
891	FSL	Feb. $\sigma$ Leonids	337.0	172.8	5.7	31.8	2.41	0.294	0.878	300.3	337.0	3.4	29	46
892	MCN	March Centaurids	352.1	218.3	-31.3	61.4	110.	0.326	0.998	110.3	172.1	137.4	6	8
893	EOP	eta Ophiuchids	358.0	260.3	-16.4	71.6	999	0.953	1.010	203.5	358.0	168.4	15	56
894	JMD	June $\mu$ Draconids	82.4	252.7	54.8	22.4	4.63	1.001	0.783	194.2	82.4	33.5	27	40
895	OAB	Oct. $\alpha$ Comae Berenicids	215.5	200.6	21.7	43.4	32.5	0.333	0.990	70.4	215.4	56.5	2	8
896	OAT	130 Taurids	179.3	86.5	17.9	72.4	999	0.996	1.107	9.9	-0.7	170.7	8	21
897	OUR	Oct. $\alpha$ Ursae Minorids	215.3	38.8	86.1	41.0	999	0.908	1.008	214.0	215.3	65.6	3	15
898	SGP	Sept. $\gamma$ Piscids	166.9	351.6	3.7	32.1	16.3	0.393	0.976	283.6	166.9	8.3	19	26
899	EMC	$\epsilon$ Microscopiids	76.2	319.8	-34.3	57.5	3.78	0.338	0.911	113.7	256.2	131.8	29	37
900	BBO	beta Bootids	289.7	229.1	45.0	47.3	9.36	0.979	0.895	174.1	289.7	81.1	72	72
901	TLC	34 Lyncids	183.4	128.1	47.2	61.4	11.4	0.696	0.939	111.7	183.4	125.0	1	1/9
902	DCT	delta Cetids	202.1	38.5	1.2	32.7	3.40	0.314	0.907	116.1	22.1	18.8	19	41
903	OAT	Oct. $\alpha$ Triangulids	206.9	30.2	28.5	28.8	2.52	0.400	0.841	288.1	206.9	17.1	4	19
904	OCO	omicron Columbids	198.3	79.4	-31.8	42.1	2.92	0.834	0.715	52.7	18.3	74.4	13	15
905	MXD	March $\xi$ Draconids	342.1	273.7	57.7	28.0	2.69	0.985	0.635	169.6	342.0	46.5	5	12
906	ETD	eta Draconids	339.5	245.6	59.6	28.9	2.86	0.973	0.660	196.7	333.7	47.6	31	72
907	MCE	mu Cepheids	132.3	316.2	56.4	32.2	2.35	0.927	0.606	219.7	132.3	55.4	7	23
908	XXL	xi2 Librids	254.4	223.0	-10.6	42.3	2.17	0.052	0.976	23.4	254.4	25.5	1	14
909	SEC	September $\epsilon$ Columbids	183.1	82.5	-38.3	42.5	3.83	0.971	0.747	21.5	3.1	74.7	17	24
910	BTC	beta2 Cygnids	40.7	292.0	30.1	51.9	10.2	0.987	0.903	194.8	40.7	93.5	51	92
911	TVU	21 Vulpeculids	43.4	303.7	30.0	52.7	5.67	0.981	0.827	173.3	43.4	97.6	36	99
912	BCY	beta Cygnids	26.2	291.4	27.8	52.9	6.86	0.992	0.855	172.3	26.2	96.9	52	127
913	FVI	41 Virginids	344.9	194.2	13.3	30.5	1.36	0.272	0.800	309.3	344.9	26.4	2	7*
914	AGE	alpha Geminids	261.9	112.7	30.1	12.2	1.21	0.826	0.436	317.2	261.9	4.1	18	-
915	DNO	delta Normids	333.7	237.7	-45.7	67.7	999	0.986	1.001	353.3	153.7	137.5	5	6*
916	ATH	April 21 Herculis	39.1	247.1	8.1	42.5	39.9	0.366	0.991	286.3	39.1	55.8	6	8
917	OVI	o Virginids	202.5	179.2	10.8	36.4	1.53	0.125	0.919	34.1	202.5	24.5	4	6*
918	TAG	theta Aurigids	154.7	90.2	34.3	66.1	999	0.578	1.005	98.3	154.7	156.9	5	21
919	ICN	iota Centaurids	301.1	199.0	-38.9	63.9	4.42	0.980	0.778	352.7	121.1	130.5	5	19
920	XSC	xi Scorpiids	50.6	237.8	-11.2	27.5	2.47	0.437	0.823	284.9	50.6	9.1	22	43
921	JLC	July $\lambda$ Capricornids	124.7	329.1	-8.5	37.3	2.49	0.129	0.950	322.7	124.7	9.8	25	49
922	PPE	Aug. $\phi$ Pegasids	137.0	356.6	20.6	56.2	28.6	0.278	0.990	297.3	137.0	117.7	3	14
923	FBO	15 Bootids	30.9	213.1	11.2	27.5	17.9	0.640	0.964	254.9	30.9	18.9	3	9
924	SAN	62 Andromedids	196.7	37.9	46.1	16.8	0.82	0.396	0.516	320.7	196.6	21.0	19	32
925	EAN	eta Andromedids	181.9	12.4	21.8	38.2	11.7	0.248	0.978	301.5	181.9	28.7	8	13
926	OMH	October $\mu$ Hydrids	196.0	154.5	-18.7	46.7	16.5	0.294	0.982	244.8	16.0	69.8	2	9

\*) Compact shower.

longitude interval from 98 to 120°. The phi Phoenicids (IAU#769, PPH) is the strongest of all the new showers detected to date by the SAAMER survey. The shower lasts for 23 days and is part of the south toroidal source. These meteoroids move in a steeply inclined ( $i \sim 74.8^\circ$ ) orbits with short semi-major axis ( $a \sim 1.26$  AU) and low eccentricity

( $e \sim 0.291$ ), having Tisserand parameter  $T_j \sim 4.4$ . Just next to this shower a second shower was discovered now named the zeta Phoenicids (IAU#768, ZPH). The shower lasts for 13 days. Those meteoroids move also in a steeply inclined orbit ( $i \sim 76.9^\circ$ ), but have longer semi-major axis ( $a \sim 2.14$  AU) and higher eccentricity ( $e \sim 0.616$ ), with Tisserand

Table 3

As Table 2, for showers previously reported to the Meteor Data Center, but not included in Jenniskens et al. (2016a).

#	IAU	Name	Sol. (°)	RAg (°)	DECg (°)	Vg (km/s)	a (AU)	q (AU)	e	$\omega$ (°)	$\Omega$ (°)	i (°)	N	Nt
648	TAL	22 Aquilids	25.0	288.0	4.0	65.4	9.77	0.980	0.900	193.6	25.0	135.7	311	524
661	OTH	110 Herculids	50.3	279.0	19.7	51.1	43.6	0.694	0.986	248.1	50.2	89.7	44	77
665	MUC	May epsilon Cygnids	58.7	319.1	29.6	57.1	11.0	1.001	0.909	168.6	58.7	107.7	31	67
672	HNJ	June 9 Herculids	75.0	243.0	4.3	18.0	2.73	0.805	0.704	239.9	75.0	12.7	23	37
677	FCL	43 Camelopardalids	75.1	117.5	74.8	16.9	2.58	0.930	0.640	142.1	75.1	21.7	33	54
679	MUA	mu Aquariids	76.0	212.7	-6.5	62.4	25.5	0.370	0.988	286.5	76.0	152.5	60	101
685	JPS	June beta Pegasus	96.0	349.6	28.4	63.5	11.8	1.011	0.914	188.5	96.0	128.9	13	28
686	JRD	June rho Draconids	82.5	298.4	67.9	35.0	57.6	1.009	0.982	170.9	82.5	55.8	10	16
687	KDP	kappa Delphinids	108.5	310.9	7.8	42.4	7.79	0.272	0.964	299.5	108.5	56.8	7	10
693	ANP	August nu Perseids	149.0	54.7	40.7	67.1	12.1	1.005	0.917	171.2	149.0	144.4	68	182
698	AET	August eta Taurids	147.5	52.5	26.8	72.9	Inf.	1.009	1.230	183.4	147.5	167.3	27	52
702	ASP	August 78 Perseids	156.1	354.2	28.0	42.8	5.22	0.296	0.944	297.1	156.1	62.8	8	11
704	OAN	omicron Andromedids	152.8	344.9	39.2	41.3	6.32	0.546	0.915	267.7	152.8	64.5	396	761
721	DAS	December alpha Sextantids	251.7	150.5	0.6	71.7	Inf.	0.913	1.073	31.0	71.7	161.3	9	16
722	FLE	15 Leonids	250.1	144.9	31.1	66.3	68.5	0.626	0.993	254.6	250.1	146.9	19	57
728	PGE	phi Geminids	276.5	118.7	22.9	37.7	3.86	0.174	0.956	313.3	276.5	4.6	6	16
730	ATV	April theta Virginids	39.3	195.2	-4.8	13.2	2.14	0.868	0.594	185.2	84.9	0.8	31	41
737	FNP	59 Perseids	125.4	69.5	45.0	57.0	20.9	0.367	0.984	73.1	125.4	117.8	24	46
745	OSD	October 6 Draconids	189.9	181.9	71.4	42.7	7.53	0.932	0.876	148.9	71.9	71.9	58	142
747	JKL	January kappa Leonids	287.6	141.9	21.5	39.5	1.75	0.078	0.955	332.7	287.6	22.8	133	--
748	JTL	January theta Leonids	311.3	165.5	12.5	40.2	1.75	0.067	0.962	334.6	311.3	23.1	107	--

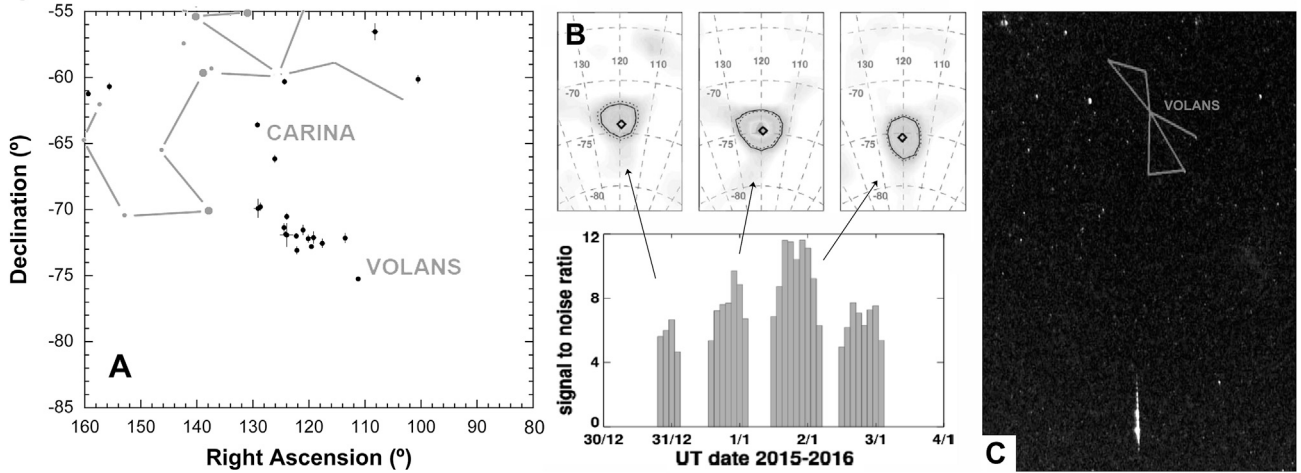


Fig. 3. The Volantids. (A) CAMS New Zealand-detected meteors in the night of December 31, 2015 (Jenniskens et al., 2016c); (B) Wind radar detections from Younger et al. (2016); (C) Photographic detected Volantid by the Desert Fireball Network (courtesy of Phil Bland and Hadrien Devillepoix).

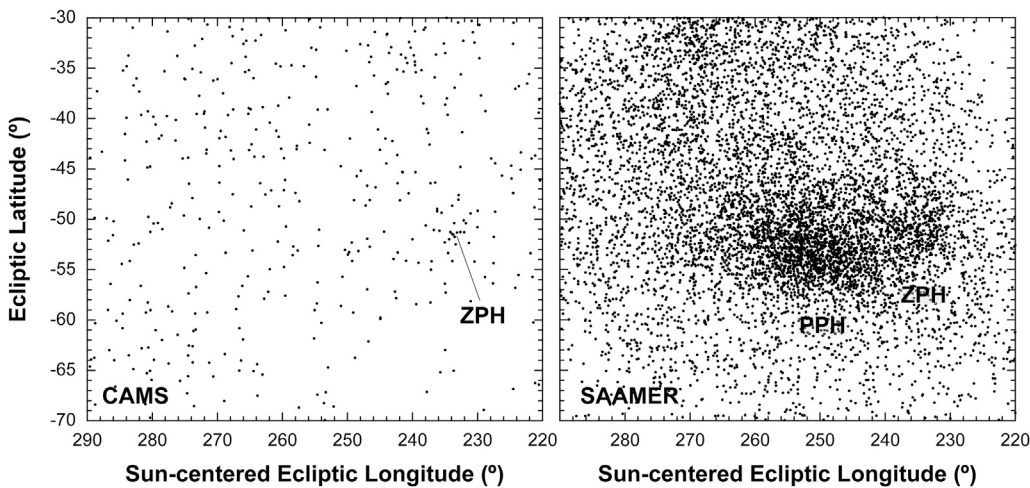


Fig. 4. CAMS (left) and SAAMER (right) detected meteors in the solar longitude interval 98–120°. The phi Phoenicids (PPH) and zeta Phoenicids (ZPH) are marked.

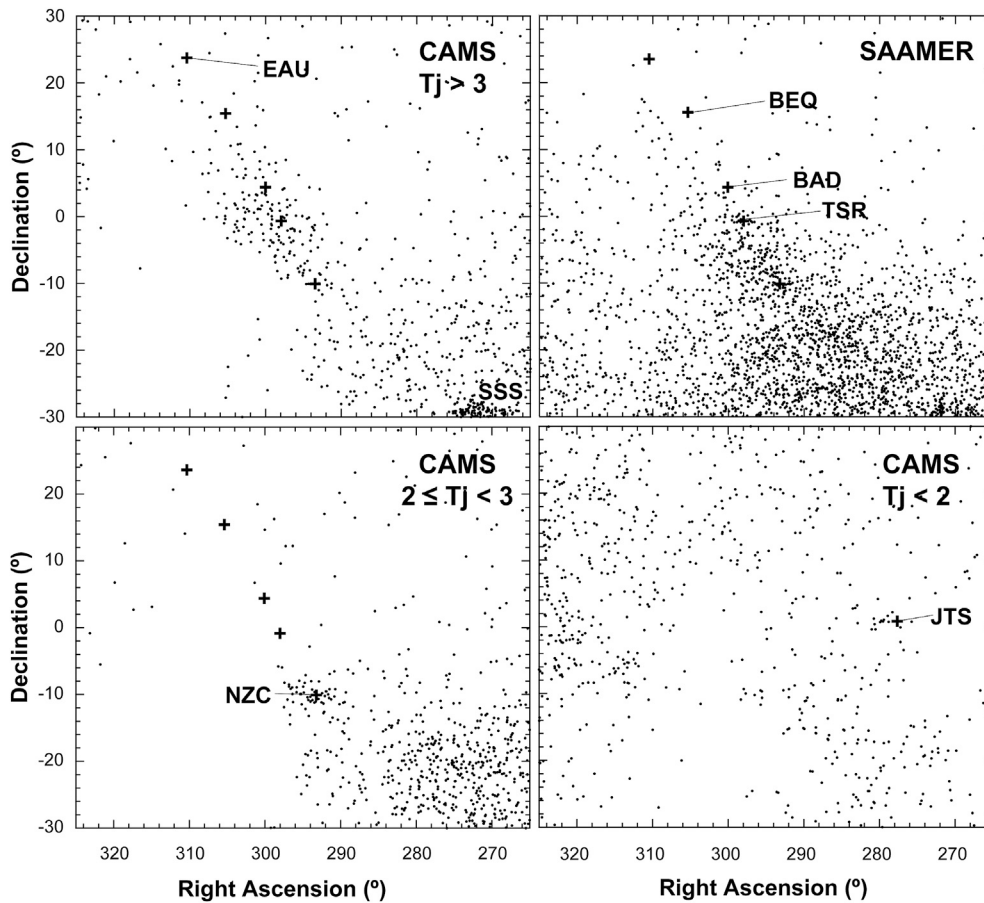


Fig. 5. Meteors detected in solar longitude interval  $80\text{--}87^\circ$ . SAAMER-detected meteors (top right panel) are plotted with the expected radiant position at that longitude of the beta Equuleids (#327, BEQ), beta Aquillids (#766, BAD), and theta Serpentids (#361, TSR). CAMS detected meteors are split in three intervals of Tisserand parameter with respect to Jupiter. The radiant position of the epsilon Equuleids (#151, EAU), Northern June Aquillids (#164, NZC), Southern sigma Sagittariids (#168, SSS), and June theta Serpentids (#683, JTS) are shown.

parameter  $T_j \sim 2.0$ .

CAMS New Zealand data show no trace of the low eccentricity phi Phoenicids, but do detect the more eccentric zeta Phoenicids (Fig. 4). The CAMS-detected orbits have nearly the same inclination ( $i \sim 78.3^\circ$ ), but higher semi-major axis (3.72 AU) and higher eccentricity ( $e \sim 0.780$ ). CAMS also detected a long-period comet shower, the June theta Serpentids (#683, JTS), not detected by SAAMER (Fig. 5).

The difference in eccentricity for different ZPH particle size suggests an evolutionary effect from Poynting-Robertson drag. P-R drag typically circularizes orbits of small particles faster than those of larger particles. The absence of phi Phoenicids in CAMS data could mean that large particles have not yet evolved into Earth-crossing orbits, or that the larger particles are lost from the stream by disintegrating more efficiently over time than small particles. The latter explanation is consistent with a rapid fading of meteoroid stream spatial density implied by the nodal distribution of CAMS-detected showers relative to that of their parent objects (Jenniskens et al., 2016a).

The prevalence of toroidal showers in radar data, previously thought to reflect a higher collisional cross section for  $q \sim 1$  AU orbits with Earth (Campbell-Brown, 2008; Vokrouhlicky et al., 2012; Pokorny and Vokrouhlicky, 2013) or thought to be a result of the Kozai cycle (Wiegert et al., 2009; Pokorny et al., 2014), could be a manifestation of this evolution. When the orbits circularize, low-inclined orbits will result in a lower relative speed with Earth, making the meteoroids more difficult to detect. Instead, highly inclined orbits continue to result in a high 30–40 km/s entry speed. That makes toroidal showers a good probe of the long-term evolution of meteoroid streams.

#### 4.2. Towards a look-up table for shower assignments

We have seen that radars may detect different showers than video

cameras, and even when both systems detect the same shower, its meteoroids can be spatially distributed differently at smaller sizes. These results require a more careful approach to meteor shower assignments by keeping a record of how particle orbits are dispersed (e.g., median position and standard deviation) as a function of particle size.

One example of the complicated task at hand is shown in Fig. 5, which displays meteors detected during solar longitude  $80\text{--}87^\circ$  at the time of newly reported shower #766, the beta Aquillids (BAD). As SAAMER's northern most detected new shower, this shower is also in the field of view of northern hemisphere surveys.

Fig. 5 shows that this meteoroid stream is dispersed in radiant coordinates and forms an elongated structure. The average position reported is just north of the densest part of the shower. An average orbit does not truly represent the shower assignment.

CAMS-detected meteors during this solar longitude interval are shown in three panels in Fig. 5, split into three groups of Tisserand parameter with respect to Jupiter. The top left panel shows meteoroids with asteroid-like  $T_j > 3$  orbits, in the same category as most radar orbits. A dense concentration of meteoroids with short semi-major axis is observed possibly slightly off-set from the radar-detected meteors.

Initially, we suspected that the beta Aquillids (BAD) shower is the same as the epsilon Aquillids (#151, EAU) reported from radar observations (Sekanina, 1976) and previously also detected in video data (Jenniskens, 2006). They stand out as having short semi-major axis ( $a \sim 0.8$  AU) orbits. Alternatively, they could be the same shower as the more recently reported beta Equuleids (#327, BEQ) or theta Serpentids (#361, TSR) from CMOR data (Brown et al., 2008).

Indeed, the BAD ( $\lambda_o = 83^\circ$ ) appear to fill the gap between TSR ( $\lambda_o = 65^\circ$ ) and BEQ ( $\lambda_o = 107^\circ$ ). Without a good understanding of how the radiant positions for the BEQ are distributed at a given time, it is difficult to establish whether it makes sense to extrapolate the activity

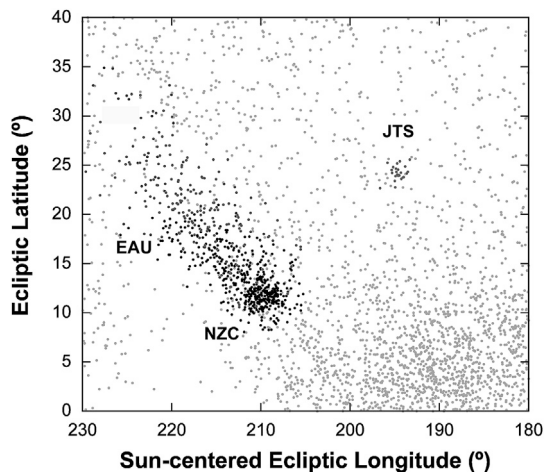


Fig. 6. Combined data of all video-based networks (CAMS, SonotaCo, Edmond and CMN) for the period of activity of the June theta Serpentids (JTS): solar longitude interval 81–94°. Shower-assigned meteors are plotted darker.

period to earlier in time than those reported from radar observations.

Brown et al. (2010) pointed out that the beta Equuleids are part of the radar-detected lambda Lyrids complex, which includes the showers lambda Lyrids (#349, LLY) around  $\lambda_0 = 41^\circ$  (284, +29), May Vulpeculids (#356, MVL) around  $\lambda_0 = 54^\circ$  (287, +23), epsilon Aquilids around  $\lambda_0 = 59^\circ$  (285, +16), theta Serpentids around  $\lambda_0 = 65^\circ$  (284, +6) and the beta Equuleids around  $\lambda_0 = 107^\circ$  (322, +9).

At the bottom-right side of this group, a shower called the Northern June Aquilids (NZC) can be found. In CAMS data, this shower stands out as having Jupiter-family comet type orbits with  $2 \leq T_j < 3$  (lower left panel). Brown et al. (2010) assigned the Northern June Aquilids (77–117°, peak at 101.5°) to a different complex. However, the parameters  $U$  and  $\cos(\Theta)$  are not invariant under P-R drag.  $U$  differentiates mostly among semi-major axis and  $\cos(\Theta)$  is the radial position in the toroidal ring. The fact that CAMS orbits for the NZC tend to have higher semi-major axis  $a = 1.74 \pm 0.01$  (0.65,  $1\sigma$ ) than those observed by SAAMER  $a = 1.46 \pm 0.21$  (Pokorny et al., 2017), albeit not as extremely so as for the ZPH, implies that longer semi-major axis showers such as the NZC could conceivably belong to the more evolved component.

Fig. 6 shows the same area in all combined video data used for the look-up table. Again it appears that the NZC belong to the same complex and are simply spread both to higher and to lower ecliptic latitudes. We chose to assign all video-detected meteors in the structure North-East of the NZC to the NZC, but introduced a separate designation (“component”) for some of the meteors. Specifically, we chose to assign the lowest IAU-numbered “EAU” to the low perihelion distance and high latitude elongation of the CAMS meteoroid distribution just north of the NZC. A more detailed comparison of radar and CAMS data is needed to understand if this choice, rather than using “TSR”, “BEQ” or “BAD”, is justified.

## 5. Conclusions

Video-based orbit surveys detect many different meteoroid streams than the current radar-based surveys. 44 new southern hemisphere showers are reported here. At least 200 southern hemisphere showers still remain to be discovered in video-based surveys, if there are as many showers on the southern hemisphere as there are on the northern hemisphere.

The duration of shower activity and the extend of the radiant distribution are all captured better in a look-up table than in the list of average orbital elements of a given shower. Each shower entry in the IAU Working List of Meteor Showers ought to be linked to the trajectory and orbital data of the detected meteoroids on which the shower assignment was based.

Future efforts will be focused on improving the CAMS shower look-up table. The new CAMS data visualization tool has the ability to show what specific meteors were assigned to a given shower in the current look-up table for any given day in the year. Where improvements are needed, this table can be modified to correct possible mistaken identities, add newly identified showers, or to improve how a shower is separated from the sporadic background.

## Acknowledgements

We thank Regina Rudawska of the IAU Meteor Data Center for checking the meteor shower nomenclature. The CAMS visualization tool was developed as part of NASA’s Frontier Development Lab 2017, a research accelerator for applying machine learning techniques. The CAMS orbital survey and this study are supported by the NASA Near Earth Object Observation program and by the University of Canterbury. The SAAMER shower orbital survey is supported by the NASA Solar System Observations program.

## Appendix A. Supplementary data

The meteor shower look-up table related to this article can be found at <https://doi.org/10.1016/j.pss.2018.02.013>.

## References

- Brown, P., Weryk, R.J., Wong, D.K., Jones, J., 2008. A meteoroid stream survey using the Canadian Meteor Orbit Radar I. Methodology and radiant catalogue. *Icarus* 195, 317–339.
- Brown, P., Wong, D.K., Weryk, R.J., Wiegert, P., 2010. A meteoroid stream survey using the Canadian Meteor Orbit Radar II: identification of minor showers using a 3D wavelet transform. *Icarus* 207, 66–81.
- Campbell-Brown, M.D., 2008. High resolution radiant distribution and orbits of sporadic radar meteoroids. *Icarus* 196, 144–163.
- Ellyett, C.D., Keay, C.S.L., 1956. Radio echo observations of meteor activity in the southern hemisphere. *Aust. J. Phys.* 9, 471–480.
- Ellyett, C., Keay, C.S.L., Roth, K.W., Bennett, R.G.T., 1961. The identification of meteor showers with application to southern hemisphere results. *MNRAS* 123, 37–50.
- Galligan, D.P., 2001. Performance of the D-criteria in recovery of meteoroid stream orbits in a radar data set. *MNRAS* 327, 623–628.
- Galligan, D.P., 2003. Radar meteoroid orbit stream searches using cluster analysis. *MNRAS* 340, 899–907.
- Galligan, D.P., Baggaley, W.J., 2004. The orbital distribution of radar-detected meteoroids of the Solar system dust cloud. *MNRAS* 353, 422–446.
- Galligan, D.P., Baggaley, W.J., 2005. The radiant distribution of AMOR radar meteors. *MNRAS* 359, 551–560.
- Gatrel, G., Elford, W.G., 1975. Southern hemisphere meteor stream determinations. *Aust. J. Phys.* 28, 591–620.
- Janches, D., Close, S., Hormaechea, J.L., Swarnalingam, N., Murphy, A., O’Connor, D., Vandepeer, B., Fuller, B., Fritts, D.C., Brunini, C., 2015. The Southern Argentina Agile Meteor Radar orbita system (SAAMER-OS): an initial sporadic meteoroid orbital survey in the southern sky. *APJ (Acta Pathol. Jpn.)* 809, 36–52.
- Jenniskens, P., 2006. *Meteor Showers and Their Parent Comets*. Cambridge University Press, Cambridge, U.K, 790 pp.
- Jenniskens, P., Gural, P.S., Dynneson, L., Grigsby, B.J., Newman, K.E., Borden, M., Koop, M., Holman, D., 2011. CAMS: cameras for Allsky Meteor Surveillance to establish minor meteor showers. *Icarus* 216, 40–61.
- Jenniskens, P., Nénon, Q., Gural, P.S., Albers, J., Haberman, B., Johnson, B., Morales, R., Grigsby, B.J., Samuels, D., Johannink, C., 2016a. CAMS newly detected meteor showers and the sporadic background. *Icarus* 266, 384–409.
- Jenniskens, P., Baggaley, W.J., Crumpton, I., Aldous, P., 2016b. Confirmation of the delta mensids (IAU#130, DME). *JIMO* 44, 187–189.
- Jenniskens, P., Baggaley, W.J., Crumpton, I., Aldous, P., Gural, P.S., Samuels, D., Albers, J., Soja, R., 2016c. A surprise southern hemisphere meteor shower on New Year’s Eve 2015: the Volantids (IAU#758, VOL). *JIMO* 44, 35–41.
- Jenniskens, P., 2017. Meteor showers in review. *Planet. Space Sci.* 143, 116–124.
- Jopek, T.J., Kanuchova, Z., 2017. IAU Meteor Data Center - the shower database: a status report. *Planet. Space Sci.* 143, 3–6.
- Jopek, T.J., Koten, P., Pecina, P., 2010. Meteoroid stream identification amongst 231 southern hemisphere video meteors. *MNRAS* 404, 867–875.
- McIntosh, R.A., 1935. An index to southern hemisphere meteor showers. *MNRAS* 95, 709–718.
- Molau, S., Kerr, S., 2014. Meteor showers on the southern hemisphere. *JIMO* 42, 68–75.
- Nilsson, C.S., 1964. A southern hemisphere radio survey of meteor streams. *Aust. J. Phys.* 17, 205–256.
- Pokorny, P., Vokrouhlicky, D., 2013. Öpik-type collision probability for high-inclination orbits: targets on eccentric orbits. *Icarus* 226, 682–693.

- Pokorny, P., Vokrouhlicky, D., Nesvorny, D., Campbell-Brown, M., Brown, P., 2014. Dynamical model for the toroidal sporadic meteors. *Astrophys. J.* 789, 25–45.
- Pokorny, P., Janches, D., Brown, P.G., Hormaechea, J.L., 2017. An orbital meteoroid stream survey using the Southern Argentina Agile MEteor Radar (SAAMER) based on a wavelet approach. *Icarus* 290, 162–182.
- Reid, I.M., Younger, J., 2016. In: Roggemans, A., Roggemans, P. (Eds.), 65 years of Meteor Radar Research at Adelaide. Proc. International Meteor Conference, Egmond, the Netherlands. June 2–5, 2016, pp. 242–246.
- Rogers, L.J., Keay, C.S.L., 1993. Observations of some southern hemisphere meteor showers. In: Stohl, J., Williams, I.P. (Eds.), *Meteoroids and Their Parent Bodies*. Proceedings of the International Astronomical Symposium Held at Smolenice, Slovakia, July 6–12, 1992. Astronomical Institute, Slovak Academy of Sciences, Bratislava, pp. 273–276.
- Sekanina, Z., 1976. Statistical model of meteor streams. IV - a study of radio streams from the synoptic year. *Icarus* 27, 265–321.
- Valsecchi, G.B., Jopek, T.J., Froeschle, C., 1999. Meteoroid stream identification: a new approach - I. theory. *MNRAS* 304, 743–750.
- Vokrouhlicky, D., Pokorny, P., Nesvorny, D., 2012. Öpik-type collision probability for high-inclination orbits. *Icarus* 219, 150–160.
- Wiegert, P., Vaubaillon, J., Campbell-Brown, M.D., 2009. A dynamical model of the sporadic meteoroid complex. *Icarus* 201, 295–310.
- Weiss, A.A., 1955. Radio echo observations of meteors in the southern hemisphere. *Aust. J. Phys.* 8, 148–166.
- Weiss, A.A., 1960. Radio-echo observations of southern hemisphere meteor shower activity from 1956 december to 1958 august. *MNRAS* 120, 387–403.
- Wiess, A.A., 1960. Southern hemisphere meteor shower activity in july and august. *Aust. J. Phys.* 13, 522–531.
- Younger, J.P., Reid, I.M., Vincern, R.A., Holdwirth, D.A., Murphy, D.J., 2009. A southern hemisphere survey of meteor shower radiant and associated stream orbits using single station radar observations. *MNRAS* 398, 350–356.
- Younger, J., Reid, I., Murphy, D., 2016. Radar observations of the Volantids meteor shower. In: Roggemans, A., Roggemans, P. (Eds.), Proc. International Meteor Conference, pp. 352–357. Egmond, the Netherlands 2-5 June 2016.